Comparison of electronic and geometric structures of nanotubes with subnanometer diameters: A density functional theory study

C. Kamal and Aparna Chakrabarti
Raja Ramanna Centre for Advanced Technology, Indore 452013, India
(Received 20 March 2007; revised manuscript received 4 July 2007; published 14 August 2007)

All-electron calculations based on density functional theory have been carried out to study the electronic structures of single-walled nanotubes with subnanometer diameters. Present studies suggest the need for performing *all-electron* calculations, specifically for the nanotubes with very small diameters. Complete geometry optimization is found to be very crucial for predicting the electronic properties. We report here the electronic properties of two of the smallest single-walled carbon nanotubes (SWCNTs)—an armchair (2,2) and a zigzag (4,0) SWCNT—with comparable diameters of about 3 Å. It is observed that, both geometrically and electronically, they are quite different. The discussion on the properties of zigzag $(n,0)$ SWCNTs, with diameters in the subnanometer regime, as a function of n, involves the elucidation of their geometric and band structures. In the band structures, systematic variations of a *nearly-free-electron-like state* and a *nearly-dispersion-free state* are shown as a function of n and their implications have been discussed. The Fermi surfaces calculated for the metallic SWCNTs show signature of a collection of quasi-Fermi-points. This shows the quasi-one-dimensional nature of these nanotubes (NTs). From the present calculations, it is expected that the number of conduction channels is restricted between 2 and 3 for the NTs studied here.

DOI: 10.1103/PhysRevB.76.075113 PACS number(s): 71.15.Mb, 73.63.Fg, 73.22.−f, 61.46.Fg

I. INTRODUCTION

The recent interest in understanding the nanostructures, including nanotubes (NTs) and nanowires, of carbon, silicon, and other semiconducting materials can be attributed to the advances in the modern methods of synthesis and the real possibility of preparing these nanostructures. The NTs are a typical class of materials in the nanoscale, and their properties can be altered controllably and significantly. Carbon nanotubes are well studied in many of their physical properties, and these materials show great potential as building blocks for nanoscale devices.[1–4] Hybrid structures of these nanomaterials with other materials are also of immense interest. It has been established from *ab initio* calculations that transition metal and nanotube hybrid structures can be made to exhibit substantial magnetism.[5,6]

The carbon nanotubes of diameter as large as a few tens of nanometers are rather well known since the discovery of the NTs,[7] but with the advancement of the method of their preparation, nowadays fabrication of smaller NTs with subnanometer diameters is possible. Very recently, freestanding single-walled carbon nanotubes (SWCNTs) of small diameter were successfully grown on small catalyst particles deposited on porous materials.[8,9] It is expected and observed that the structural, electronic, and optical properties of NTs with small diameter, in the subnanometer range, are quite unusual compared to those of the NTs with large diameter. Due to the severe curvature effect in the NTs with small diameter, the detailed understanding of the microscopic properties of these small diametered tubes is very important. The interesting and often unique structural and electronic properties observed in the NTs with small diameter as well as the recent opportunities of studying them microscopically from the advanced theoretical techniques led to many "computer experiments" on these materials recently.[1,10–19]

Independent studies on band structures and the geometric structures based on first-principles calculations of many of the SWCNTs (studied here) exist in the literature.[1,10,14,15,18,19] However, so far as our knowledge goes, systematic comparison and detailed studies of various geometric and electronic properties of SWCNTs, with subnanometer diameters, as a function of curvature or the wrapping indices, using *all-electron* calculational method have not been carried out. Hence the importance of the present study lies on the following few aspects. Since carbon is an element from the first row of the Periodic Table, the present *all-electron* calculations probe if there is any significant disagreement between the *all-electron* and previous pseudopotential calculations, and hence, if the necessity for *all-electron* calculations for these small tubes can be established. Our studies suggest the need of using *all-electron* calculations, specifically for very small tubes and complete geometry optimization. The shortcomings of the pseudopotential calculations have been shown from the detailed comparison of the electronic properties predicted by the present and previous pseudopotential calculations. This comparison hints at a possible lack of proper geometry optimization in the existing pseudopotential calculations. Further, we observe and study the systematics of a few important features of the band structures, as a function of size. The systematics for a *nearly-dispersion-free state* and a *nearly-free-electron-like state* in the band structures has been noted in this study and the implication of this has been discussed. The importance of establishing the systematics for small tubes is that it can enable us to extrapolate these results for larger tubes, based on the different trends obtained here. We also discuss here the nature of the Fermi surface observed for the metallic tubes. We then make a general observation about the typical number of conduction channels expected for these tubes.

In this paper, using state of the art *all-electron* calculations based on the density functional theory (DFT), we compare the details of the geometric and electronic properties of the two smallest NTs, namely, the armchair SWCNT(2,2)

TABLE I. Optimized geometries of different nanotubes. Distances (d1 and d2) are in angstrom and angles (a1 and a2) are in degrees.

Material	Diameter	d1	d2	a1	a2
SWCNT(2,2)	2.93	1.44	1.46	111.6	111.6
SWCNT(4,0)	3.39	1.40	1.49	107.0	119.5
SWCNT(5,0)	4.25	1.39, 1.40, 1.43	1.45, 1.48, 1.49	110.3, 110.6	119.4, 119.9
SWCNT(6,0)	4.82	1.40	1.44	112.9, 113.5	120.2
SWCNT(7,0)	5.56	1.41	1.43	115.0	120.0
SWCNT(8,0)	6.28	1.41	1.42	115.3–115.6	120.1, 120.6
SWCNT(9,0)	7.05	1.42	1.42	116.2	120.4

and zigzag SWCNT(4,0), both with comparable diameter of about 3 Å. Systematic variation of geometric and electronic properties of the SWCNTs and their implication as well as possible application, as a function of n for the zigzag SWCNT(n,0)s, have also been discussed in detail in this paper. In the next section, we discuss the method employed for the *all-electron* calculations. Section III discusses the results. Finally, in Sec. IV, we summarize the results and conclude.

II. METHOD

Optimized geometric and electronic structures of NTs made of elements of carbon, with subnanometer diameter, have been obtained from *all-electron* calculations based on density functional theory.[20] For *all-electron* calculations, WIEN97 code[21] has been used to perform the *ab initio* relativistic full potential linearized augmented plane wave calculations using generalized gradient approximation [22] for the exchange correlation. In calculations of SWCNTs, a minimum energy cutoff of 15 Ry has been used. The cutoff for charge density was $G_{\max}=14$. The muffin-tin radius was taken to be 1.3 a.u. for C. The number of k points for self-consistent field cycles is taken such that it resulted in a minimum of 102–208 k points in the irreducible part of the Brillouin zone (BZ). The calculations were performed with the convergence criterion for total energy (E_{tot}) to be less than 0.1 mRy. All the parameters for the calculations have been used after optimizing them with respect to the electronic properties of the materials. A supercell geometry is assumed, where in one direction the nanotube is periodic, and hence, infinitely long; this direction is called the tube axis. In the other two directions, a vacuum region, spanning about 12 Å, has been used so that the interaction between two adjacent tubes in the periodic arrangement is negligible. The structures are optimized by minimizing the Hellmann-Feynmann forces until the forces on individual atoms are small (below 5 mRy/a.u.).

III. RESULTS AND DISCUSSION

A. Geometric structure

We study the optimized geometric structures of SWCNT(2,2) and SWCNT(n,0), with n being 4–9. The numbers in the parentheses denote the wrapping indices of the nanotube, obtained after rolling a two-dimensional single layer graphitic (graphene) sheet.[2,3] The unit cell of armchair tube (2,2) and zigzag tube (n,0) contains 8 and 4n atoms, respectively. For carbon, the values of bond length and bond angles in graphene (sp^2 hybridization) and in diamond (sp^3 hybridization) are taken as 1.42 Å, 120° and 1.54 Å, 109.47°, respectively. The starting value of the bond length is taken after a graphenelike structure with sp^2 hybridization.

We optimize the geometric structures of all the nanotubes. Table I shows the diameters as well as the values of nearest neighbor bond lengths and bond angles for the optimized structures. The relaxed structures of carbon nanotubes show two types of bond length (denoted by d1 and d2, see Fig. 1) and bond angle (denoted by a1 and a2, see Fig. 1). The geometric structures of SWCNT(2,2) and SWCNT(4,0) are compared here. Due to the armchair structure, the SWCNT(2,2) has a different definition of bond length d1 as is clear from Fig. 1. d1 in the armchair case is a C-C bond along the tube ring and perpendicular to the tube axis. In the case of zigzag tubes, d1 is parallel to the tube axis. The sp^2 type character is prevalent in the former case in terms of the bond lengths, with two different bond lengths d1 and d2 being 1.44 and 1.46 Å, which are somewhat closer to the sp^2 value of 1.42 Å. However, the bond angle of 111.6° matches better with that corresponding to the sp^3 hybridization. On the contrary, as is evident from Table I, there is a distribution in the bond length with respect to the starting value in the case of SWCNT(4,0). d1 and d2 are 1.40 and 1.49 Å. a1 and a2 are 107° and 119.5°. These values clearly indicate a stronger mixture of the sp^2 and sp^3 hybridizations in this case.

Next we discuss the effect of size (diameter) or curvature on the geometric structure of the zigzag nanotubes. For the

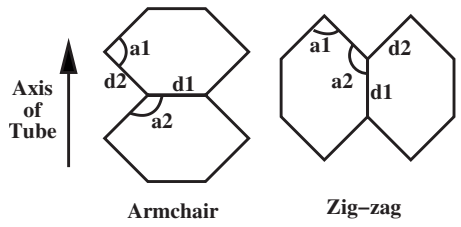

FIG. 1. Two types of bond lengths (d1 and d2) and bond angles (a1 and a2) are shown in both armchair and zigzag tubes. Axis of tube is marked with an arrow. a1 is the angle between two d2 bond lengths, and a2 is between d1 and d2 in the case of both the armchair and zigzag tubes.

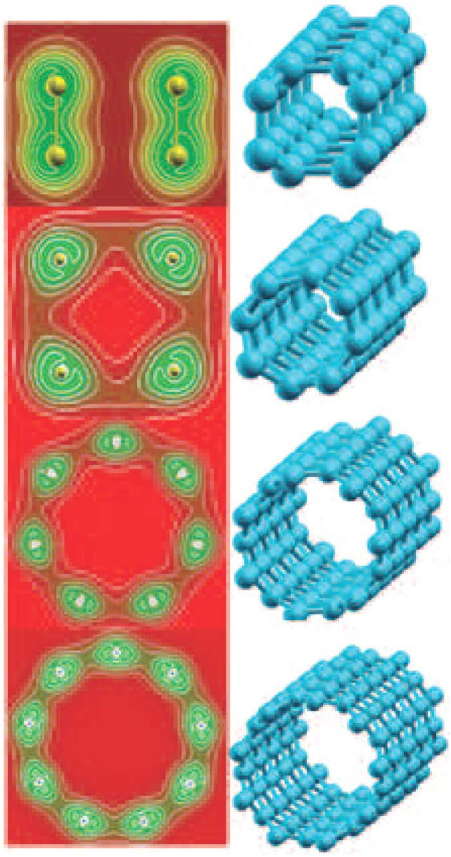

FIG. 2. (Color online) A part of the armchair tube SWCNT(2,2) along with its valence charge density (in left panel) is shown in the top row. Below, part of zigzag tubes with $n=4$, 7, and 9 (from second to last row, respectively) are also shown along with their valence charge densities (in left panel).

zigzag $(n,0)$ tubes with smaller diameter, the bond along the axis of the tube (d1) gets shortened, whereas the other bond (d2) gets enlarged (see Fig. 1 and Table I). This effect is prevalent when tube diameter is smaller.[1] The increase in bond length (d2) and decrease in bond angles (a1) indicate substantial contribution from sp^3, in addition to sp^2 hybridization, for SWCNT with n less than and around 7. Conversely, for tubes with n greater than and around 7 for carbon, the bond lengths and bond angles are very similar to that of a graphenelike structure, indicating more contribution from sp^2 rather than from sp^3. This signifies that the curvature effect in larger tubes is less predominant as is indicated from the valence charge density plots as well (discussed below).

B. Electronic structure

1. Valence charge density

Figure 2 shows the valence charge density distribution of the carbon nanotubes, (2,2), (4,0), (7,0) and (9,0), calculated in the plane perpendicular to tube axis using XCRYSDEN package.[23] We compare the valence charge densities for the SWCNT(2,2) and (4,0). The geometry of SWCNT(2,2) is such that there are two σ bonds (d1 type) on the plane perpendicular to the tube axis. This can be easily seen from the valence charge distribution. However, in the case of SWCNT(4,0), there are no σ bonds on the plane perpendicular to the tube axis. Hence, while the SWCNT(4,0) has a strong asymmetry in charge distribution inside and outside the tube, (2,2) shows a different charge distribution. From the geometry discussion above also, it is evident that the SWCNT(4,0) has a stronger mixture of sp^2 and sp^3 hybridizations than the (2,2) case (see Table I). Figure 2 also gives the valence charge densities of SWCNT(7,0) and SWCNT(9,0). Our results match well with previous studies.[18] When we compare the zigzag tubes, SWCNT$(n,0)$ with different n, an asymmetry in the distribution of valence charge density inside and outside the tubes becomes evident. This effect is more pronounced as the tube diameter decreases and n becomes less than and around 7. This is due to the fact that, as the tube diameter decreases, the overlap between the π orbitals (inside the tube) and σ orbitals (on the surface of the tube) increases. Hence, the valence charge redistribution between π and σ orbitals arises and the tubes are not in sp^2 hybridization as expected from the band folding scheme, but a mixture of both sp^2 and sp^3, as discussed above.

2. Band structure

In the present work, we calculate the band structures (BSs) of SWCNTs with small diameters using *all-electron* method. The electronic structures of nanotubes have been explained earlier by a simple band folding picture, where it has explicitly been assumed that the σ orbitals are orthogonal to π orbitals. However, this is a very simplified picture because when the diameter of the tube is small, then the σ orbitals are no longer orthogonal to the π orbitals.[3,10] Therefore, simple band folding scheme does not predict the electronic structure of small tubes correctly. In the present work, we do a systematic study of all the band structures for SWCNT$(n,0)$, for $n=4-9$. These have been obtained using the *all-electron* calculations[21] to study the difference in their various features with respect to the pseudopotential calculations. Figure 3 depicts some of the band structures of the $(n,0)$ nanotubes, n being even (6 and 8) and odd (7 and 9) numbers. Figures 4–6 give the electronic band structures of SWCNT(2,2), SWCNT(4,0), and SWCNT(5,0), respectively, without and with geometry optimization. The band structures are plotted along the high symmetry points (along the axis of the tube).

Figures 3–6 show that all the other nanotubes are metallic except SWCNT with $(n,0)$, n being 5 and 7–9. According to the simple band folding scheme, SWCNT(4,0), SWCNT(5,0), SWCNT(7,0), and SWCNT(8,0) should be semiconductors and SWCNT(2,2), SWCNT(6,0), and SWCNT(9,0) are metallic. However, it is generally observed that there are some disagreements with this simple scheme. We find that while SWCNT(4,0) is metallic, SWCNT(9,0) is semiconducting, with a very small gap. For bigger tubes, with n greater than or equal to 6, *all-electron* results on the electronic nature and the overall band structure of the tubes agree reasonably well with the previous pseudopotential

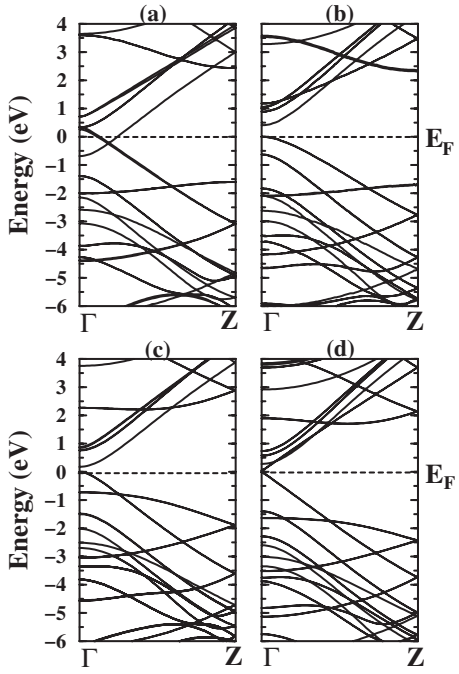

FIG. 3. Band structures of (a) SWCNT(6,0), (b) SWCNT(8,0), (c) SWCNT(7,0), and (d) SWCNT(9,0). The Fermi energy is shown by a dashed line. The band energies are normalized with respect to the Fermi level.

calculations.[15,17,19] SWCNT(6,0) is a metallic case. The band structure of SWCNT(7,0) (Fig. 3) shows that the tube is a semiconductor with a band gap of 0.19 eV. There is an energy gap of about 0.43 eV in the case of SWCNT(8,0), while in the case of SWCNT(9,0), although it is expected to be metallic, a very small gap (0.07 eV) opens up. These values agree well with the earlier reported values.[15,17,19]

All-electron versus pseudopotential calculations. For smaller tubes, where data are available, namely, for (2,2) and (5,0) SWCNTs, the electronic nature of the material as well as the details of the band structures turn out to be different

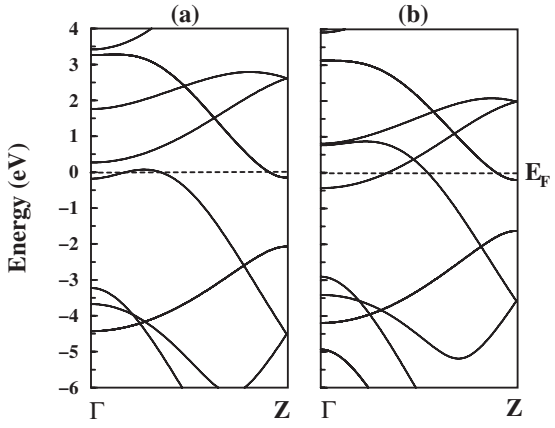

FIG. 4. Band structures of (a) SWCNT(2,2) without geometry optimization and (b) SWCNT(2,2) with geometry optimization. The Fermi energy is shown by a dashed line. The band energies are normalized with respect to the Fermi level.

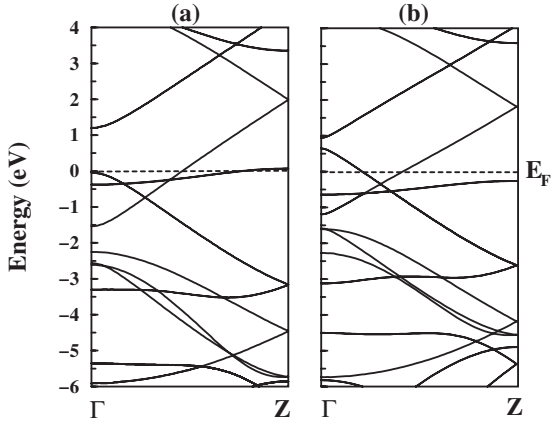

FIG. 5. Band structures of (a) SWCNT(4,0) without geometry optimization and (b) SWCNT(4,0) with geometry optimization. The Fermi energy is shown by a dashed line. The band energies are normalized with respect to the Fermi level.

from the pseudopotential calculations.[14,18] Figure 6 contains the electronic structures of SWCNT(5,0) before and after geometry optimization. From *all-electron* calculation, the unrelaxed geometry corresponds to a metallic nature of this tube. However, even with geometry optimization, previous pseudopotential calculations obtain a metallic nature.[18] However, in our calculations, when the geometry is optimized, a band gap appears, thus making the fully relaxed tube a semiconductor. In addition, opening up of a band gap is clearly observed when it is plotted as a function of decreasing residual force, averaged on the different carbon atoms (Fig. 7). We also note that for the SWCNT(2,2), while the existing pseudopotential calculations[14] report that it is an indirect band gap semiconductor, the present calculations predict a metallic nature (Fig. 4). When the present band structure without geometry optimization is compared with the pseudopotential calculations, we find that these band structures are rather similar, specifically near the Fermi level. Similarly, while SWCNT(4,0) is found to be metallic both ways, its BS in Fig. 5 exhibits differences in the band structures with and

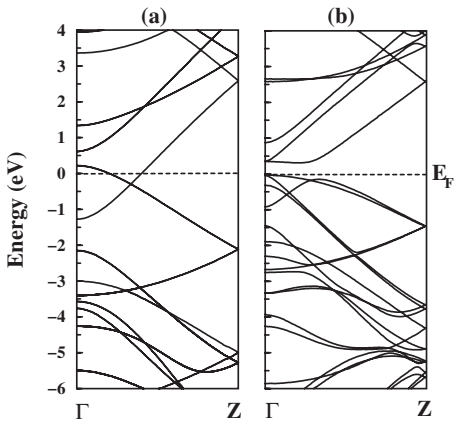

FIG. 6. Band structures of (a) SWCNT(5,0) without geometry optimization and (b) SWCNT(5,0) with geometry optimization. The Fermi energy is shown by a dashed line. The band energies are normalized with respect to the Fermi level.

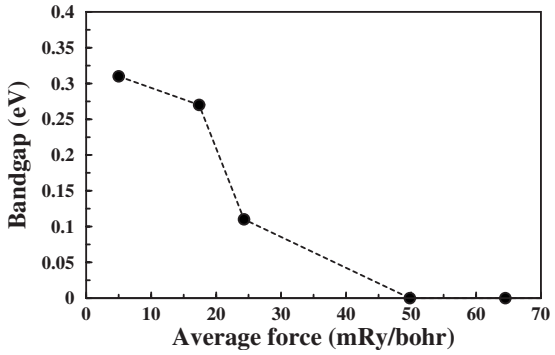

FIG. 7. Band gap of SWCNT(5,0) as a function of the residual force, averaged over different carbon atoms. The dashed line is a guide for the eye.

without optimization, specifically around the Fermi level.

The above-mentioned observations hint at a possible lack of proper geometry optimization in the pseudopotential calculations.[14,18] We note that for smaller tubes, the starting and final optimized geometries (Table I) are quite different. Moreover, due to the smaller size of the tubes, the steric hindrance at places is much more and atoms can interact strongly along the diameter since the size is very small. Hence obtaining the global equilibrium structure in the smaller tubes is difficult. On the contrary, for larger NTs, both starting and final optimized geometries are close to that of the sp^2 hybridized ones. So optimization of geometry is expected to be easier. We know that the role of geometry optimization is very crucial for obtaining the correct properties: we observe that the discrepancy between the pseudopotential and present calculations is greater for the smaller tubes compared to the larger ones, due to the reasons discussed above. Hence it is suggested from the present study that, for electronic structure of SWCNTs of ultrasmall diameters, the *all-electron* calculations seem to be the method of choice. The reason for the shortcomings of the pseudopotential calculations may lie on the choice of parameters, namely, the energy cutoff or the choice of the potential itself, which may have led to insufficient optimization of geometry for the very small tubes.

Detailed comparison of the BS of SWCNT(2,2) and SWCNT(4,0). Now we compare the electronic structure of the two smallest tubes. Due to larger curvature effect, π orbital overlaps with the σ orbital, which pushes down some of the band toward the Fermi level and makes SWCNT(4,0) metallic. The metallicity of the armchair SWCNT(2,2) tube, however, does not change due to curvature because the shift in the wave vector is parallel to an allowed line of the nanotube, and hence, armchair SWCNT(2,2) remains metallic even in the modified band folding scheme.[3] When the band structure of the SWCNT(2,2) is compared with the same one obtained from pseudopotential-based DFT calculations,[14] it is observed that the bands below the Fermi level from both studies are in reasonable agreement.[14] However, while this pseudopotential study predicted an indirect band gap for the (2,2) case, present calculations yield a metallic nature. Though the band structure from the present study shows that the SWCNT (4,0) is metallic as it is in case of SWCNT(2,2), there are certain features which make the two cases very different in their properties. When the band structure of the SWCNT(2,2) is compared with that of the SWCNT(4,0), of very similar diameter, the dispersion of the bands around the Fermi level is found to be quite different. While for the latter, the dispersion of the bands near the Fermi level is more of linear type, the former has it otherwise.

Signature of the nearly-dispersion-free states. Unlike the case of SWCNT(2,2), the electronic structure of SWCNT(4,0) is observed to have an interesting feature of existence of a few localized types of bands at energy values close to the Fermi level. This indicates an accumulation of a large density of states (DOS) at these energy values. Notably, the *nearly-dispersion-free* states (denoted hereafter as NDF states) closely below the Fermi level may have special significance, in terms of the Van Hove singularity in the DOS. One of these localized bands which is very near the Fermi level (the band energy at the Γ point is about -0.65 eV with respect to the Fermi level), can become important due to the possibility of a large *DOS at the Fermi level* [denoted hereafter as $N(E_F)$] as a result of hole doping, under the rigid-band model. The important consequence may be altered optical and electronic properties in the case of doped SWCNT(4,0).

Furthermore, from the band structure calculations of the $(n,0)$ NTs, we observe that, in the SWCNTs with even-numbered n, signature of such NDF state exists, as is observed in the case of (4,0), but they are further deep down in energy with respect to the Fermi level. On the contrary, from the band structures of the $(n,0)$ SWCNTs with odd values of n, it is noticed that their band structures are rather similar and that there is a notable absence of NDF states below the Fermi level in these materials. However, in the energy region above Fermi level, the signature of a band being flat appears. An atom and orbital projected band analysis indicates that for both the odd and even n cases, the contribution is from the p orbitals of carbon. It is expected that in the even n case, it is the contribution of the occupied part of the $2p$ orbitals, while in the odd n case, it is the contribution of the unoccupied part.

Figure 8(a) shows the plot of the two band energy values of these NDF states, one at the Γ point and the other at the Z point; the energy values are normalized with respect to E_F. Their difference is also plotted and has values around zero. It is noticed that with increasing n, both these energy values decrease overall, with alternating signs (due to odd and even n) and a sawtooth structure. Our analysis indicates that for some particular value of n (some value greater than 9), there may be a possiblity of a significant accumulation of DOS at the Fermi level. This accumulation can happen for a smaller tube as well. For example, in the case of SWCNT(4,0), as a result of hole doping, a large $N(E_F)$ is possible under the rigid-band model.

Systematics of the nearly-free-electron-like states. It is observed that there is a signature of a band with a parabolic type dispersion above the Fermi level in all the cases studied. This is termed as a *nearly-free-electron-like* state (denoted hereafter as NFE state) in the literature.[24] Nanotubes are hierarchical solids like C_{60} with an unusual space inside the solid.[24] In the case of NTs, the free space is near the center of

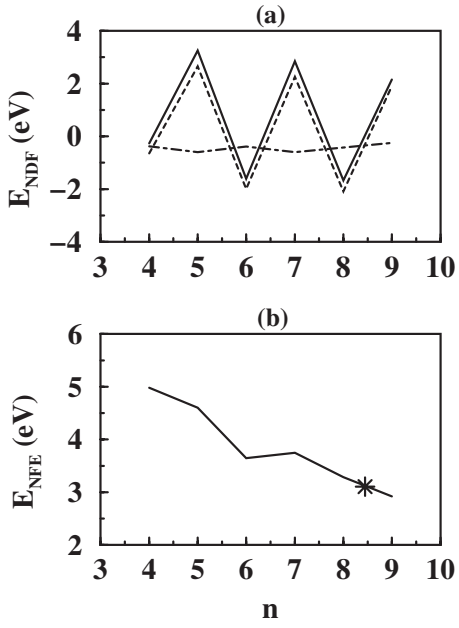

FIG. 8. Energies of the (a) *nearly-dispersion-free* states and (b) *nearly-free-electron-like* states as a function of n, the wrapping index. In (a), the solid line and the dashed line correspond to the energies, normalized with respect to E_F, at the Z point and Γ point, respectively. The dot-dashed line corresponds to the difference between these two energies. In (b), the energy of the *nearly-free-electron-like* state for graphene is indicated by a star.

the tube and away from the tube surface. Hence, near the center of the tube, the electrons can be in the near-free state giving rise to this NFE state, which will have important implication in the electronic-transport properties of these tubes. The band picture of armchair SWCNT(2,2) and zigzag SWCNT(4,0) shows that the NFE state is around 3.91 and 4.98 eV, respectively, above the Fermi level at the Γ point of the BZ. In Fig. 8(b), we plot the energy corresponding to the NFE state [denoted hereafter by E(NFE)] at the Γ point as a function of n. The E(NFE) has been normalized with respect to Fermi level. For $n \leqslant 9$, there is a downward and linear trend in the E(NFE) value with increasing n, and hence, the diameter of the tube.

It is observed from the energy plots of the *nearly-free-electron-like* state as a function of n that the E(NFE) value for graphene falls near the E(NFE) value for $n=8$. It is hence expected that the graphitic nature is expected more in tubes with n value around 7 or 8, and hence, the curvature effect in these tubes is less predominant. From the linear nature of the E(NFE) versus n curve in Fig. 8(b), it is indicated that there may exist a possibility that for some value of n, say, n', which is larger than 9, the NFE state can be at energy $E=E_F$. When the data in Fig. 8(b) are linearly extrapolated, this n' value turns out to be around 16, with the diameter of the tube of about 12 Å. In this respect, k-resolved inverse photoemission studies can be very instructive to study the NFE states of these tubes systematically as a function of n.

3. Quasi-Fermi-points

For metallic cases, the calculation of Fermi surface is instructive since the linear response of a metal to an electric, magnetic, or thermal gradient is determined by the shape of the Fermi surface. The shape of the Fermi surface is generally derived from the symmetry, periodicity of the crystalline lattice, and occupation of the electronic energy bands. The systems under study are hexagonal networks of carbon rolled into single-walled tubes. A carbon nanotube is a one-atom-thick sheet of graphene rolled up into a cylinder with a diameter which is of the order of a nanometer. This rolling-up results in a quasi-one-dimensional nanostructure, where the ratio of length and diameter is very high. For such a quasi-one-dimensional nanostructure, the Fermi surface is expected to consist of a few points. Our calculations of the Fermi surface for all the metallic cases, at the limit of a large length and diameter ratio, exhibit a behavior of Fermi surface which can be ascribed as quasi-Fermi-points (hereafter denoted as QFP). For each case, the QFPs are obtained at the points of the BZ where a band crosses the Fermi level. This behavior clearly shows the signature of the quasi-one-dimensional nature of these NTs studied here. We note that the number of Fermi crossings corresponds to the number of conduction channels in a particular structure. We observe that for SWCNT(2,2) and (6,0), there are three bands each, which cross the Fermi level, while for SWCNT(4,0), there are two band crossings. So for the SWCNTs studied here, the number of conduction channels is expected to be restricted between 2 and 3.

IV. CONCLUSION

The most important observation of the present study involves the band structure calculations of very small tubes and the comparison of these with the same one obtained from the pseudopotential calculations. The results and discussions on electronic structures of the SWCNTs stress on the need for complete geometry optimization, and also the *all-electron* calculations seem to be the method of choice, specifically for the NTs with very small diameters.

From the geometric structure study of the SWCNT(n,0) with n varying from 4 to 9, it is observed that the curvature effect is less predominant in tubes for n being greater than and around 7. This is indicated from the valence charge density calculations as well, namely, the asymmetry of the charge distributions inside and outside the tube is more prominent for smaller tubes. From the studies on the two smallest carbon nanotubes, SWCNT(2,2) and SWCNT(4,0), it is observed that these two tubes of very close diameters are both geometrically and electronically quite different. The Fermi surface calculated for the metallic SWCNTs shows a signature of a collection of quasi-Fermi-points that, in turn, clearly shows the quasi-one-dimensional nature of these NTs. For the metallic SWCNTs under study in this paper, the number of conduction channels is expected to be restricted between 2 and 3. It is observed that the band pictures of the SWCNT(n,0)s with odd-numbered n show resemblance to each other, and the band structures of tubes with even-numbered n exhibit similar features. Both the odd and even n tubes show systematic variations of a *nearly-free-electron-like* state and a *nearly-dispersion-free* state. Under the rigid-

band model, the possibility of a large DOS at the Fermi level, as a result of moderate hole doping, exists for SWCNT(4,0), thus making it technologically important. A large density of states in the Fermi level is expected at a particular value of n, which is larger than $n=9$, due to the *nearly-dispersion-free* states. Under the rigid-band model, hole or electron doping may also give rise to a large $N(E_F)$ in the tubes under study.

ACKNOWLEDGMENTS

We thank A. K. Nath and V. C. Sahni for encouragement and support. L. M. Ramaniah is thanked for introducing us to the exciting field of nanotubes. S. R. Barman and S. Pal are acknowledged for fruitful discussions. The support and help of the scientific computing group at the Computer Centre, RRCAT, are gratefully acknowledged.

[1] S. Ciraci, S. Dag, T. Yildirim, O. Gülseren, and R. T. Senger, J. Phys.: Condens. Matter **16**, R901 (2004), and references therein.
[2] M. S. Dresselhaus, G. Dresselhaus, and P. Avouris, *Carbon Nanotubes: Synthesis, Structure, Properties and Applications* (Springer-Verlag, Berlin, 2001).
[3] S. Reich, C. Thomsen, and J. Maultzsch, *Carbon Nanotubes: Basic Concepts and Physical Properties* (Wiley-VCH, Weinheim, 2004).
[4] R. H. Baughman, A. A. Zakhidov, and W. A. de Heer, Science **297**, 787 (2002).
[5] C. K. Yang, J. Zhao, and J. P. Lu, Phys. Rev. Lett. **90**, 257203 (2003).
[6] A. K. Singh, T. M. Briere, V. Kumar, and Y. Kawazoe, Phys. Rev. Lett. **91**, 146802 (2003).
[7] S. Iijima, Nature (London) **354**, 56 (1991).
[8] T. Hayashi, Y. A. Kim, T. Matoba, M. Esaka, K. Nishimura, T. Tsukada, M. Endo, and M. S. Dresselhaus, Nano Lett. **3**, 887 (2003).
[9] C. Maryn, M. D. Serrano, N. Yao, and A. G. Ostrogorsky, Nanotechnology **14**, L4 (2003).
[10] X. Blase, L. X. Benedict, E. L. Shirley, and S. G. Louie, Phys. Rev. Lett. **72**, 1878 (1994).
[11] O. Gulseren, T. Yildirim, and S. Ciraci, Phys. Rev. B **65**, 153405 (2002).
[12] H. J. Liu and C. T. Chan, Phys. Rev. B **66**, 115416 (2002).
[13] X. Zhao, Y. Liu, S. Inoue, T. Suzuki, R. O. Jones, and Y. Ando, Phys. Rev. Lett. **92**, 125502 (2004).
[14] Y. L. Mao, X. H. Yan, Y. Xiao, J. Xiang, Y. R. Yang, and H. L. Yu, Phys. Rev. B **71**, 033404 (2005).
[15] V. Zolyomi and J. Kurti, Phys. Rev. B **70**, 085403 (2004), and references therein.
[16] R. Barnett, E. Demler, and E. Kaxiras, Phys. Rev. B **71**, 035429 (2005).
[17] Y. Miyamoto, A. Rubio, X. Blase, M. L. Cohen, and S. G. Louie, Phys. Rev. Lett. **74**, 2993 (1995).
[18] T. Miyake and S. Saito, Phys. Rev. B **68**, 155424 (2003); **72**, 073404 (2005).
[19] G. Chen and Y. Kawazoe, Phys. Rev. B **73**, 125410 (2006).
[20] P. Hohenberg and W. Kohn, Phys. Rev. **136**, B864 (1964); W. Kohn and L. J. Sham, *ibid.* **140**, A1133 (1965).
[21] P. Blaha, K. Schwartz, and J. Luitz, WIEN97, Technische Universitaet, Wien, Austria, 1999.
[22] J. P. Perdew, K. Burke, and M. Ernzerhof, Phys. Rev. Lett. **77**, 3865 (1996).
[23] A. Kokalj, Comput. Mater. Sci. **28**, 155 (2003); J. Mol. Graphics Modell. **17**, 176 (1999); A. Kokalj and M. Causa, Proceedings of High Performance Graphics Systems and Applications European Workshop, Bologna, Italy, 2000, pp. 51–54.
[24] S. Okada, A. Oshiyama, and S. Saito, Phys. Rev. B **62**, 7634 (2000).